Journal of Rock Mechanics and Geotechnical Engineering 6 (2014) 156–164

Contents lists available at ScienceDirect

Journal of Rock Mechanics and Geotechnical Engineering

journal homepage: www.rockgeotech.org

Anisotropy of strength and deformability of fractured rocks

Majid Noorian Bidgoli*, Lanru Jing

Department of Land and Water Resources Engineering, Engineering Geology and Geophysics Research Group, Royal Institute of Technology (KTH), 11423 Stockholm, Sweden

ARTICLE INFO

Article history:
Received 20 November 2013
Received in revised form
15 January 2014
Accepted 22 January 2014
Available online 3 February 2014

Keywords:
Anisotropy
Strength criterion
Deformation behavior
Numerical experiments
Fractured rock mass
Discrete element method (DEM)
Discrete fracture network (DFN)

ABSTRACT

Anisotropy of the strength and deformation behaviors of fractured rock masses is a crucial issue for design and stability assessments of rock engineering structures, due mainly to the non-uniform and non-regular geometries of the fracture systems. However, no adequate efforts have been made to study this issue due to the current practical impossibility of laboratory tests with samples of large volumes containing many fractures, and the difficulty for controlling reliable initial and boundary conditions for large-scale in situ tests. Therefore, a reliable numerical predicting approach for evaluating anisotropy of fractured rock masses is needed. The objective of this study is to systematically investigate anisotropy of strength and deformability of fractured rocks, which has not been conducted in the past, using a numerical modeling method. A series of realistic two-dimensional (2D) discrete fracture network (DFN) models were established based on site investigation data, which were then loaded in different directions, using the code UDEC of discrete element method (DEM), with changing confining pressures. Numerical results show that strength envelopes and elastic deformability parameters of tested numerical models are significantly anisotropic, and vary with changing axial loading and confining pressures. The results indicate that for design and safety assessments of rock engineering projects, the directional variations of strength and deformability of the fractured rock mass concerned must be treated properly with respect to the directions of in situ stresses. Traditional practice for simply positioning axial orientation of tunnels in association with principal stress directions only may not be adequate for safety requirements. Outstanding issues of the present study and suggestions for future study are also presented.

1. Introduction

It is well-known that rock masses are very complex materials in nature, due to the existence of fractures of varying sizes, orientations and mechanical properties, so that their mechanical behaviors are discontinuous, inhomogeneous, anisotropic, and not linearly elastic (DIANE). Anisotropy is defined as variations of properties with respect to the directions concerned in design and analysis of rock structures. A rock mass is often considered as anisotropic because mainly it contains the fracture system geometry that is usually not uniformly or regularly distributed, and its behavior may change with loading directions. However, how significant such change may become has not received adequate research and our basic understanding about this important issue remains unclear. Therefore, the objective of this research is quantitative demonstration and representation of the anisotropy of strength and deformability of fractured rocks due to its impact on design, safety and performance assessment of rock engineering projects.

Concept of anisotropy is well-known in the field of rock mechanics and engineering. Morland (1976) investigated elastic anisotropy of regularly jointed rock mass during a theoretical study, which was an initial effort on the influence of joint on the elastic anisotropy. Amadei and Savage (1989) and Amadei (1996) pointed out the importance of anisotropy of rock masses and discussed the interaction existing between rock anisotropy and stress, deformability and strength of a rock mass containing a regular single joint set. Experimental researches based on standard laboratory tests with small sample sizes were reported in literature about anisotropy of strength and deformability of the different rock materials, such as those given by Reik and Zacas (1978), Broch (1983), Chen et al. (1998, 2011), Yang et al. (1998), Ajalloeian and Lashkaripour (2000), Nasseri et al. (2003), Gonzaga et al. (2008), and Cho et al. (2012). Given the fact that small rock samples cannot contain fractures with varying sizes, orientations and locations at larger scales, the obtained results from such laboratory tests cannot be

* Corresponding author. Tel.: +46 8 790 8661.
E-mail address: mnoorian@kth.se (M. Noorian Bidgoli).

Peer review under responsibility of Institute of Rock and Soil Mechanics, Chinese Academy of Sciences.

Production and hosting by Elsevier

1674-7755
http://dx.doi.org/10.1016/j.jrmge.2014.01.009

representative of fractured rock masses. Sun et al. (2012) performed numerical research on anisotropy of mechanical parameters of a moderately large volume fractured rock mass, but the testing and modeling considered only the uniaxial compressive test conditions without confining pressure, so that a proper understanding on the strength and deformability of the rock mass sample concerned could not be obtained. Therefore, one of the remaining challenging issues for rock mechanics and engineering now is how to evaluate anisotropic nature of fractured rocks of realistic fracture system geometry. Since laboratory and in situ tests for fractured rock samples of large volumes are not practically possible, a comprehensive predictive numerical study is necessary for establishing conceptual understanding on the anisotropy of deformation behavior and strength of fractured rock masses.

Based on the above motivation, the main objective of this research is to predict numerically how deformability and strength of a typical fractured rock sample may vary in different loading directions of rotational computational models of fracture systems at its representative elementary volume (REV) size, since such a systematic numerical testing is rarely reported. In the context, the Young's modulus and Poisson's ratio were selected as equivalent elastic deformability. The friction angle and cohesion for Mohr–Coulomb (M–C) and parameters *m* and *s* for Hoek–Brown (H–B) criteria were selected as equivalent strength parameters, respectively. A series of fractured rock models were used to evaluate the directional variation of these parameters representing deformability and strength of the computational models, since they are most commonly applied in the field of rock mechanics and engineering.

2. Approaches of research by numerical experiments

2.1. Model establishment

As a general research approach, a systematic numerical uniaxial and biaxial test procedure was developed for observing the anisotropic behaviors of the rotated fractured rock models containing a large number of fractures of varying sizes, created using the stochastic discrete fracture network (DFN) method, based on the realistic fracture system information from field mapping, as reported in Noorian Bidgoli et al. (2013). The stress-deformation analysis was performed using the discrete element method (DEM) (Fig. 1). The obtained stresses and strains from these numerical experiments were used to fit the well-known M–C and H–B failure criteria, represented by equivalent material properties

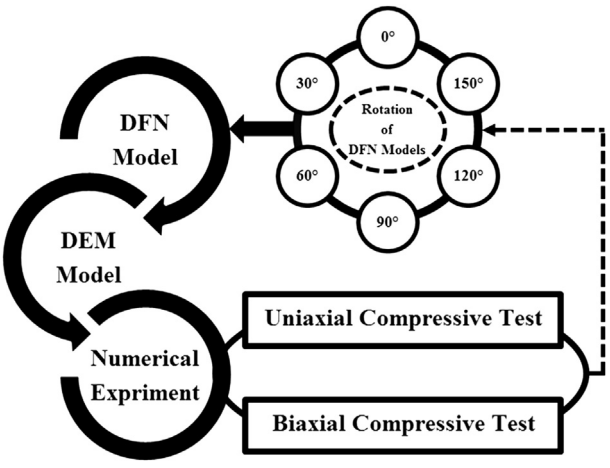

Fig. 1. Flowchart for the process of numerical experiments on strength and deformability of fractured rock models using rotational DFN models.

to define these two criteria. The equivalent Young's modulus and Poisson's ratio were derived by the stress–strain curves during the elastic deformation ranges of the whole stress–strain curves.

The rotated DFN models were defined by rotating a primary geometrical DFN model extracted from a larger DFN model (Fig. 2), from 0° to 180° with an interval of 30° in an anti-clockwise direction (Fig. 3). The size of square-shaped DFN models was 5 m × 5 m that was equal to the REV size as defined in Min and Jing (2003), which is the minimum model size beyond which the elastic mechanical properties of the models remain basically constant. The fracture system geometry data are that used in Noorian Bidgoli et al. (2013), from a site investigation mapping at the Sellafield, UK (Nirex, 1997), so that their descriptions are not included in this paper to avoid unnecessary repetitions. The mechanical parameters are described in the subsequent section during model descriptions.

The universal distinct element code, UDEC (Itasca, 2004) was used to perform numerical loading tests on fractured rock models, similar to the standard compression test on small intact rock samples in the laboratory. The computational models were established with the following assumptions:

(1) The numerical model was defined in a 2D space for a generic study.
(2) Simulations were performed under quasi-static plane strain conditions for deformation and stress analysis, without considering effects of gravity.
(3) Rock matrix was a linear, isotropic, homogeneous, elastic, and impermeable material.
(4) The fractures follow an ideal elastoplastic behavior of an M–C model in the shear direction and a hyperbolic behavior (Bandis' Law) in the normal direction.
(5) Strain-softening with continuous loading was not considered since the peak stress at the elasoplastic deformation process was required and the model behavior cannot be considered as an equivalent continuum behavior with continued strain-softening behavior.
(6) In order to highlight the effect of loading condition, due to the relatively small REV size of the fracture system, and since no groundwater flow was included in the investigation, a constant initial aperture of fractures was assumed.

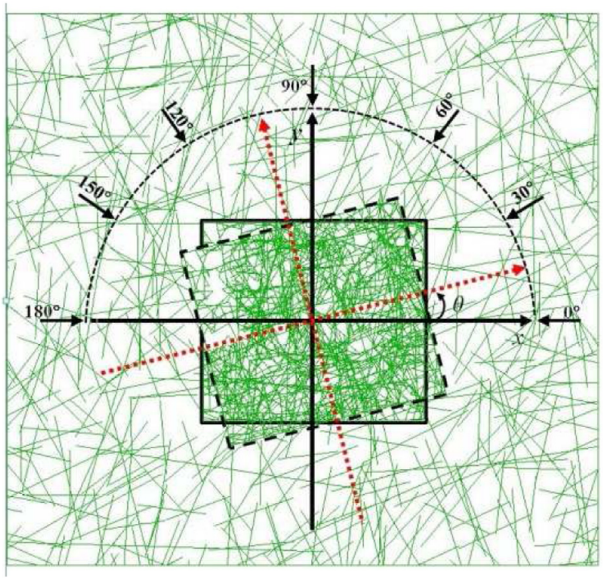

Fig. 2. Extracting a DEM model with size of 5 m × 5 m from the center of the original parent model and its rotating in various direction angles from 0° to 180° with a 30° interval.

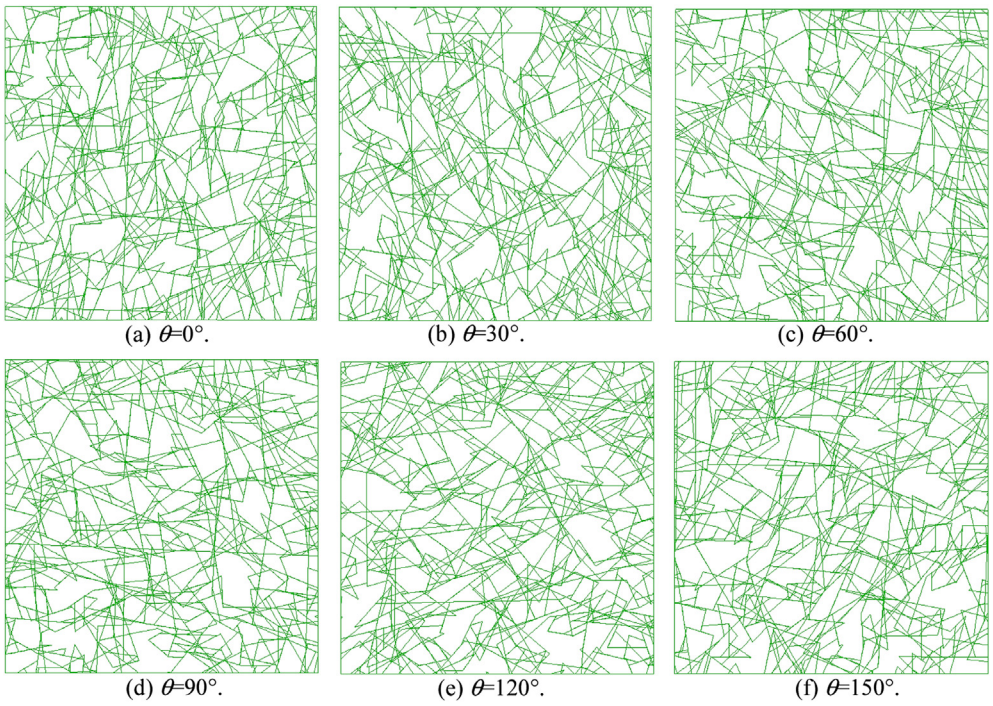

Fig. 3. Fracture system geometry of rotated DEM models in various direction angles of 0°, 30°, 60°, 90°, 120° and 150°.

The basic data used about the mechanical properties of fractured rock for modeling in UDEC are those of intact rock and fractures. The density, Young's modulus, Poisson's ratio, and uniaxial compressive strength (UCS) of intact granitic rock are 2500 kg/m^3, 84.6 GPa, 0.24 and 157 MPa, respectively. The normal stiffness, shear stiffness, friction angle, dilation angle, and cohesion of fractures were specified as 434 GPa/m, 434 GPa/m, 24.9°, 5° and 0 MPa, respectively. The mean initial aperture under zero normal stress was assumed to be 65 μm. The residual aperture at high stresses is 1 μm, and the shear displacement at which shear dilation reached a stable level is 3 mm. The above parameters, the same as those of fracture system geometry parameters, were obtained from a site investigation program of Nirex Ltd. (Nirex, 1997) and related laboratory tests, so that the DFN models as generated for this study are realistic realizations of site-specific conditions. However, these parameters were derived for representing merely the behaviors of the computer models developed for this research but not the site geological conditions.

2.2. Procedure of numerical experiments

The numerical experiments were designed for simulating conventional uniaxial and biaxial compression tests on the rotated DEM models. For the uniaxial compression test, the two vertical sides of the DEM model were kept as free surfaces and the bottom of the DEM models was fixed in the axial loading direction (i.e. the *y*-direction). An incrementally increased axial load was applied on the top of the DEM model. For the biaxial compression tests, varying confining pressures were applied on the two vertical boundary surfaces of the model and the rest of boundary conditions were the same as those for the uniaxial tests.

The numerical uniaxial and biaxial compression tests started by applying a constant axial load increment, equal to 0.05 MPa, on the top of the DEM models in the vertical direction, followed by a continued process of iteration (cycling), with the same stress increment of 0.05 MPa, until a quasi-static equilibrium state of the

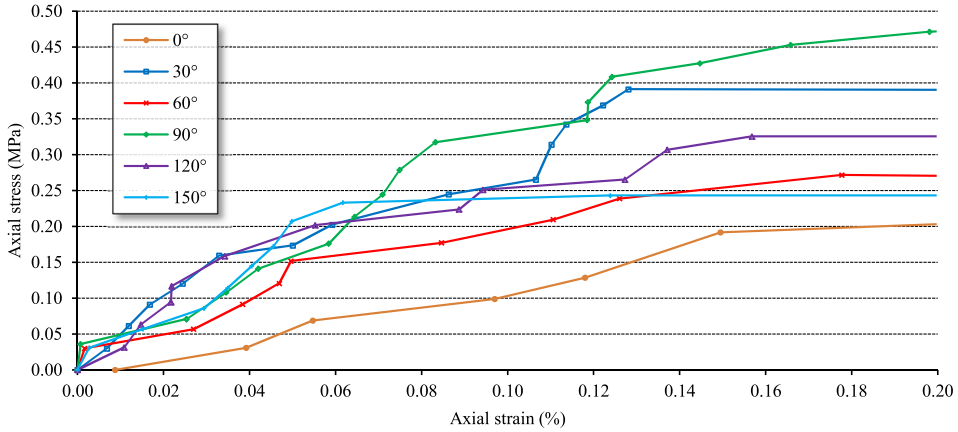

Fig. 4. Axial stress versus axial strain curves for the rotated DEM model in various direction angles, without confining pressures.

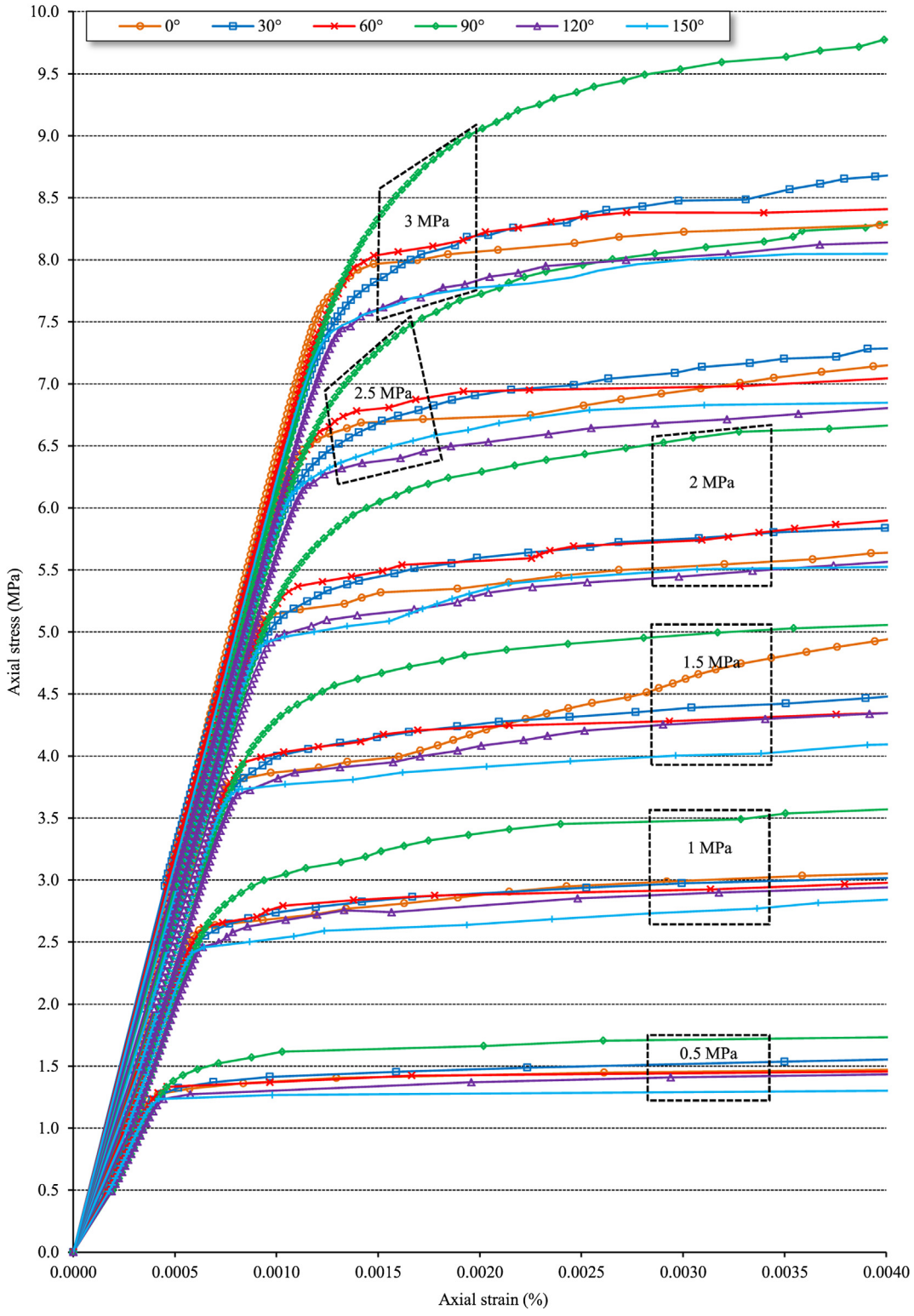

Fig. 5. Axial stress versus axial strain curves for the rotated DEM models in various direction angles of 0°, 30°, 60°, 90°, 120° and 150°, and under different confining pressures of 0.5 MPa, 1 MPa, 1.5 MPa, 2 MPa, 2.5 MPa and 3 MPa.

models was reached. The uniaxial and biaxial loadings were performed as servo-controlled loading procedures using a new FISH program in UDEC for selecting a proper cyclic loading rate in a reasonable range of maximum and minimum unbalanced forces to prevent sudden failure of the DEM models. During cycles of loading, a velocity monitoring technique was employed for checking static behaviors of the models to ensure that the velocities at a number of pre-defined monitoring points become (or very close to) zero at the end of every loading step during simulation. A grid of 36 points located at intersection points of the six parallel horizontal and six

vertical lines on the DEM models was defined, where the velocities (used for checking approaching a quasi-static steady state of the models concerned), displacements and stress components (used for calculating averaging values of stress and displacement components) were monitored during the loading processes.

For each rotated model, the numerical tests were composed by seven loading steps, through applying a set of confining pressures of 0 MPa (representing a uniaxial loading test), 0.5 MPa, 1.0 MPa, 1.5 MPa, 2.0 MPa, 2.5 MPa and 3.0 MPa, respectively. Under each confining pressure, iterative axial loading (cycling) continued with the fixed increment until a peak stress at the end of elastoplastic deformation process of the DEM models was reached. It should be noted that the equivalent strength and deformability of the fractured rocks, as equivalent continua, were the concern of research, not the complete constitutive model of the fractured rock concerned. Therefore, the loading needs to be stopped when the peak strength of the model was reached, for homogenization (averaging) of the equivalent strength parameter evaluations.

In total, 42 UDEC models (6 rotational directions and 7 loading steps) were simulated. The average values of the normal stress and strain components of each DEM model were calculated at the end of each loading step, and plotted as stress-strain curves for deriving peak strength and the elastic deformability parameters. The average values of stress and strain components of the tested model were computed as the corresponding equivalent values from the monitoring points as described above, since the model size is equal to the REV size of the fractured rocks as reported in Min and Jing (2003).

3. Results and analysis

3.1. Stress–strain curves

Figs. 4 and 5 show the curves of axial stresses versus axial strains for the rotated DEM models with 7 different confining pressures (Fig. 5), as functions of the 6 orientation angles of the models, respectively. These curves were used to evaluate strength and elastic deformability behavior of the fractured rock models, after the models reached their peak strength. Strain-softening may appear if continued axial loading was applied. The results for the uniaxial loading (Fig. 4) are exceptional since, unlike testing small samples of intact rock materials, the model of large number of blocks reached the peak strength much more quickly with larger strains with no lateral confining pressure, thus it is not appropriate to be presented in the same plot as the others.

Generally, it can be seen from the numerical results that the DEM models deform linearly and elastically during the initial loading stage with axial stresses below the yield strength (the stress point where change of elastic to plastic deformation process starts on the stress–strain curves), whose magnitudes depend on the confining pressure. Afterwards, continued axial compression then leads to inelastic deformation up to the peak strength. With increase of lateral confining pressure, the strengths of the DEM models increase and the stress–strain curves follow an elasto-plastic behavior with a strain hardening trend. Although the general deformation behavior of the DEM models had similar trends with rotation of the fractured rock models, the magnitude of peak stress and slope of stress–strain curves before reaching the yielding strength varied with rotation angles, indicating existence of anisotropy of strength and deformability, which are mathematically analyzed in the next section.

3.2. Anisotropy of the equivalent deformability parameters

Young's modulus and Poisson's ratio are two important parameters that were used to investigate the elastic deformability of rock and rock mass. The Young's modulus was calculated as the averaged slope of the stress–strain curves of the DEM models during the stage of elastic deformation, and the Poisson's ratio was calculated as the ratio of the mean transverse strain to the mean axial strain of the DEM models.

Figs. 6 and 7 show variations of the equivalent Young's modulus and Poisson's ratio as functions of rotation angles of the models with varying confining pressures. As can be seen in Fig. 6, although the equivalent Young's modulus of the fractured rock models increases gradually with the increase of confining pressures, it changes slightly with model rotation angle. Due to small values of Young's modulus near the origin of the coordinate frame (in Fig. 6), the values of Young's modulus at zero confining pressure are presented. On the other hand, as shown in Fig. 7, the equivalent Poisson's ratios of the models decrease generally with the increase of confining pressures, but with moderately more variations with model rotation angle.

In general, one may conclude that during elastic deformation process, the stress–strain behavior of the fractured rock model is basically isotropic but not linear-elastic, since the Poisson's ratio can be larger than 0.5 at certain loading conditions and model orientations.

3.3. Anisotropy of the equivalent strength of the fractured rock model

The calculated major and minor principal stress pairs (σ_1, σ_3) obtained from the numerical experiments on the rotated DEM models were utilized for evaluating changes of equivalent strength of the rotated DEM models based on the M–C and H–B criteria. The normalized versions of the M–C and H–B (Hoek and Brown, 1980) criteria can be written as the following relations between major (σ_1) and minor (σ_3) principal stresses.

For M–C criterion, we have

$$\frac{\sigma_1}{\sigma_3} = \frac{1+\sin\varphi}{1-\sin\varphi} + \frac{\frac{2c\cos\varphi}{1-\sin\varphi}}{\sigma_3} \tag{1}$$

For H–B criterion, we have

$$\frac{\sigma_1}{\sigma_3} = 1 + \sigma_{ci}\frac{\left(m\frac{\sigma_3}{\sigma_{ci}} + s\right)^{0.5}}{\sigma_3} \tag{2}$$

where c is the cohesion and φ is the friction angle, the two strength parameters defining the M–C failure criterion; m and s are the two parameters defining the H–B failure criterion; and σ_{ci} is the UCS of the intact rock.

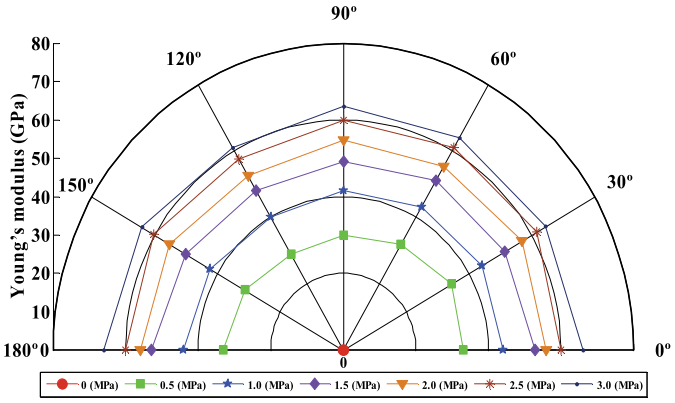

Fig. 6. Distribution of equivalent Young's moduli for the rotated DEM model in various direction angles, under different confining pressures (Young's moduli at zero confining pressure are 43 MPa, 30.7 MPa, 31.5 MPa, 35.5 MPa, 36.6 MPa and 37.6 MPa for 0°, 30°, 60°, 90°, 120° and 150° direction angles, respectively).

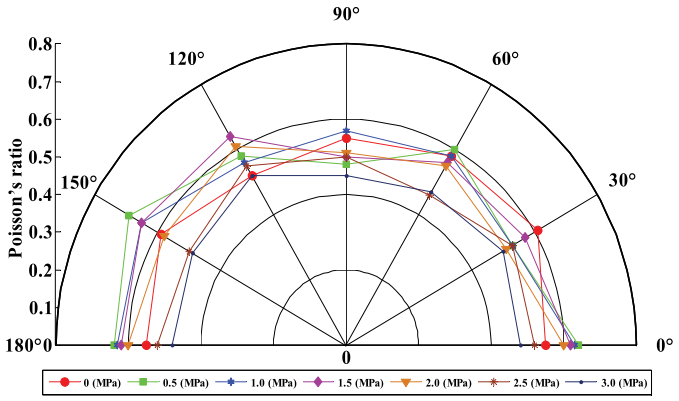

Fig. 7. Distribution of Poisson's ratios for the rotated DEM model in various direction angles, under different confining pressures.

The curve fitting results, as normalized strength versus normalized confining pressure with M–C and H–B failure criteria, are shown in Fig. 8 using data of the rotated DEM models under different confining pressures. Correlation coefficients are presented in Table 1 for each rotation angles. The fitting qualities of M–C and H–B strength envelopes were acceptable, but the M–C criterion was better for the numerical results.

For a more quantitative comparison between M–C and H–B failure criteria, a root mean squared error (RMSE) index was used as an indication of the differences between strength values predicted by two criteria and measured numerical values. The values of RMSE can be calculated as

$$\mathrm{RMSE} = \sqrt{\frac{1}{n}\sum_{i=1}^{n}\left(\sigma_{1,i}^{\mathrm{p}} - \sigma_{1,i}^{\mathrm{m}}\right)^2} \tag{3}$$

where $\sigma_{1,i}^{\mathrm{p}}$ and $\sigma_{1,i}^{\mathrm{m}}$ are the predicted and measured values of σ_1 for the ith rotated model, and n is the number of data pairs equal to 7, i.e. one pair for uniaxial and six pairs for biaxial numerical tests in this study.

Table 1
Root mean squared error (RMSE) and correlation coefficient (R) values of the M–C and H–B criteria in prediction of normalized strength.

Rotation angle of DEM models θ (°)	RMSE		R	
	M–C	H–B	M–C	H–B
0	0.284	0.555	0.9950	0.9915
30	0.393	0.826	0.9996	0.9842
60	0.249	0.730	0.9992	0.9855
90	0.447	0.986	0.9993	0.9824
120	0.199	0.694	0.9994	0.9868
150	0.481	0.755	0.9992	0.9847
Average value	0.342	0.758	0.9986	0.9858

RMSE values of the M–C and H–B failure criteria for all of model rotation angles are given in Table 1, which shows that in all of the rotated models considered, the M–C criterion showed lower RMSE magnitudes in comparison of the H–B criterion, and hence M–C strength envelope fits better with the overall mechanical behavior of the fractured rock model. This observation, however, is still subjective to the modeling conditions of this study, and conclusions may change when different fracture system geometries and mechanical properties are used.

3.4. Anisotropy of the equivalent strength parameters

Figs. 9–12 show the directional variations of equivalent cohesion c, friction angle φ, m and s of the rotated DEM model, respectively. The numerical results show a certain degree of anisotropy of the equivalent cohesion when the M–C criterion was used (see Fig. 9). The frictional angle also changes insignificantly with model rotations (Fig. 10). The small changes of the friction angle obtained were due to insignificant changes of the slope angles of the fitted linear curves in Fig. 8a, based on M–C criterion. The equivalent parameters m and s of the H–B criterion show

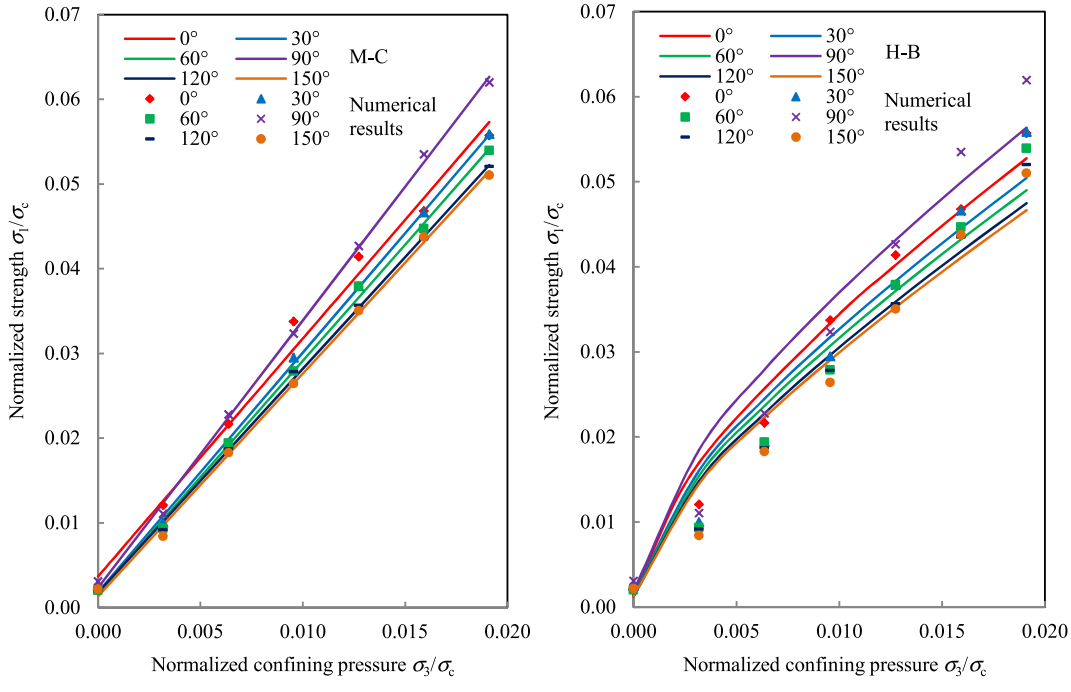

(a) M-C. (b) H-B.

Fig. 8. Strength curves for the rotated DEM models in the normalized principal stress space: (a) M–C, (b) H–B.

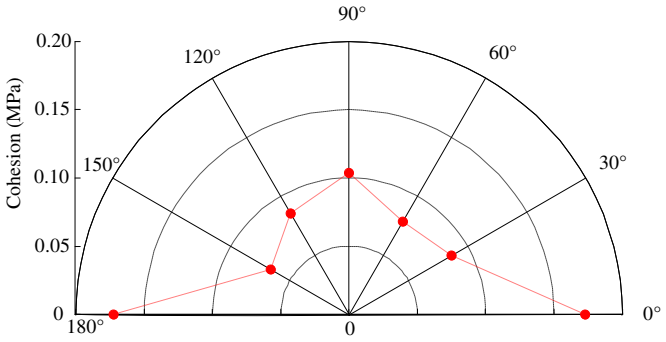

Fig. 9. Distribution of equivalent cohesion for the rotated DEM models.

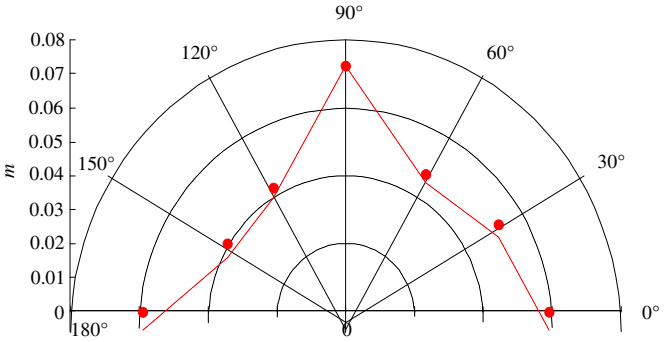

Fig. 11. Distribution of equivalent H–B parameter (m) for the rotated DEM models.

significant directional dependences (Figs. 11 and 12), especially in the directions of 150° and 90°.

In summary, one may conclude that the equivalent strengths of the models are significant, whether either M–C or H–B criteria are adopted, and major changes occur when model was oriented to 0°, 30°, 90° and 150°, respectively. This is a clear contrast with elastic deformation parameters. The main reason is that the nonlinear plastic deformation caused significant irreversible anisotropic distributions of stress and displacement fields that were largely controlled by fracture system geometry.

4. Discussions

In this study, we investigate anisotropy of strength and deformability of fractured rock masses using a predictive numerical methodology. The numerical results indicate significant anisotropy of strength and elastic deformability of fractured rocks models, which vary with the loading conditions. The main reason for such anisotropic feature of strength and deformation behaviors is the complex fracture system geometry that was not regular and isotropic, so that the model behaved differently for different model rotations, even if their loading conditions were identical.

Figs. 13 and 14 show distribution of fracture orientation angles with length more than 1 m and 2 m, respectively, as rose diagrams. One can see from these figures that numbers of fracture in the directions of 90°, 30° and 150° are more than other directions, especially when the length of fractures equals 2 m (Fig. 14). Since the main fractures of longer lengths play more significant roles in stress-displacement behaviors of the tested models, anisotropy in the strength and deformability begins to be more significant for the models rotated to these directions, because these major fractures are the major weakness planes causing major stress changes in the related directions, with respect to the loading directions.

Fig. 15 shows the iso-value contours of the minor principal stress of the DEM model with rotation angles of 150° and 90°

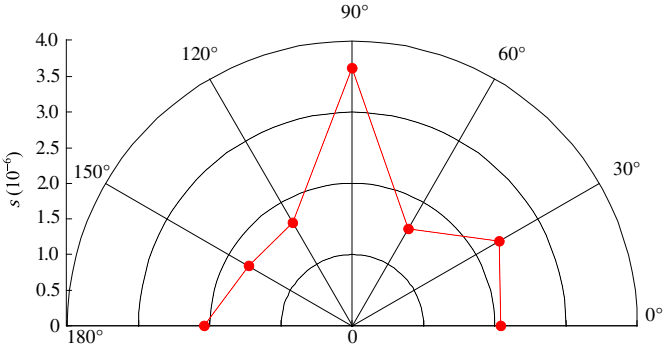

Fig. 12. Distribution of equivalent H–B parameter (s) for the rotated DEM models.

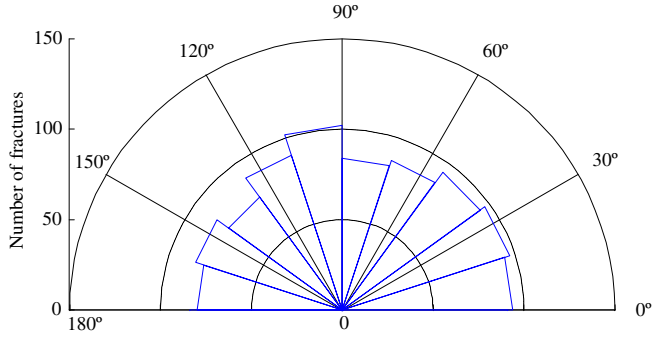

Fig. 13. Distribution of fractures with length more than 1 m over different direction ranges.

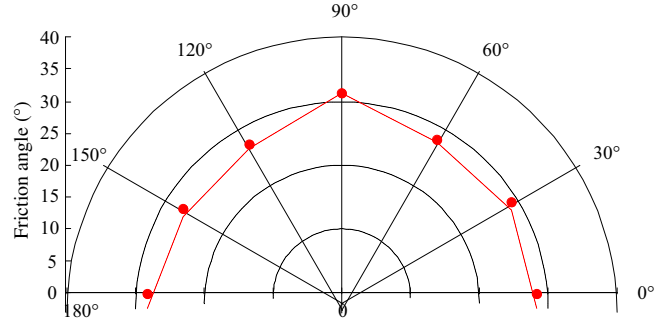

Fig. 10. Distribution of equivalent friction angle for the rotated DEM models.

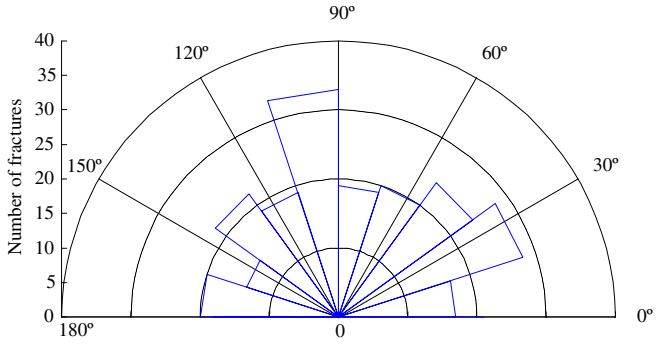

Fig. 14. Distribution of fractures with length more than 2 m over different direction ranges.

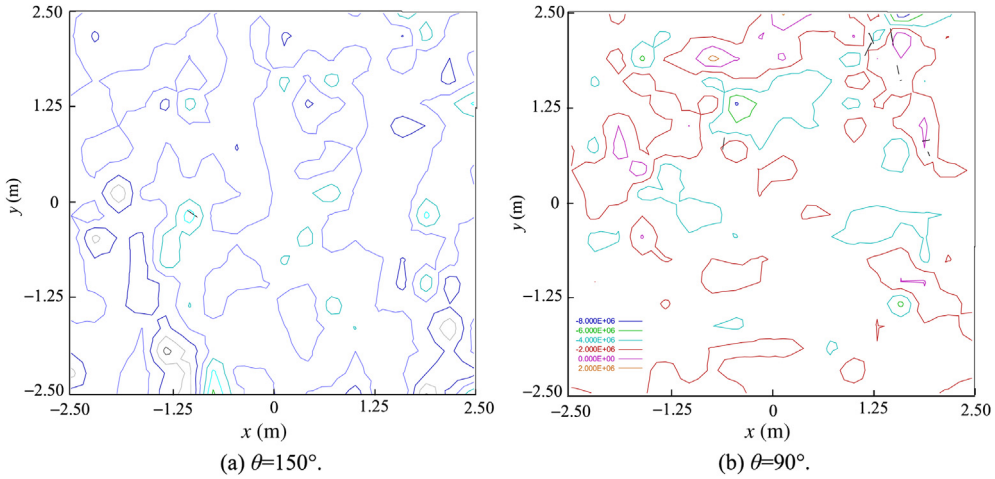

Fig. 15. Distribution of minor principal stress contours (unit: Pa) of the DEM model with (a) 150° rotation, and (b) 90° rotation.

with respect to the horizontal *x*-direction, respectively. Significant variation of stress distribution occurred, due to the different orientations of fractures relative to the directions of axial load and lateral confining pressures. In conclusion, the fractured rock displays anisotropic behaviors in strength and deformability, depending on fracture system geometry and loading directions.

5. Concluding remarks

This paper presents a systematic study for investigating anisotropy of strength and deformability of fractured rocks by a series of uniaxial and biaxial numerical compression tests on rotated 2D DEM models, which has not be attempted before. The parameters identified for demonstrating anisotropy of deformability are the equivalent Young's modulus and Poisson's ratio. The anisotropic strength envelopes were fitted by adopting the M–C and H–B criteria, respectively, from which the equivalent values of cohesion and internal friction angles (when the M–C criterion was adopted) and the parameters *m* and *s* (when the H–B criterion was adopted) were derived. The results provide an important conceptual understanding of the variation range of anisotropy of fractured rock concerned and the main reasons causing such variations. Some concluding remarks are presented below:

(1) In view of current limited small-scale laboratory tests and practical impossibility for proper controlling of large-scale in situ tests of large volumes of fractured rock masses, numerical modeling is probably the preferred method available at present for predicting the anisotropy of strength and deformability of fractured rocks.
(2) Anisotropies of strength and deformability of fractured rocks are important issues for design and performance of rock engineering projects, since the relative directions of in situ stresses (determining the loading directions), fracture system geometry (selecting the directional variation of stress distribution) and rock engineering projects (such as choosing axis of tunnels relative to not only in situ stress directions but also orientations of dominating fracture sets) may have a significant impact on the safety and performance of the rock engineering structures located in fractured rock masses.
(3) Due to the directional dependence of strength and deformability of fractured rocks, proper site investigations for in situ stress and fracture system behaviors are crucial for design and performance/safety assessments of underground engineering works in fractured rock mass.
(4) From the results obtained from the models developed in this research, both the M–C and the H–B criteria provided acceptable fitting to the numerical results of strength, with M–C criterion yielding better estimation of the RMSE values for engineering practices. More investigations are needed for understanding the physical reasons for the differences.
(5) The results demonstrate that laboratory tests of intact rock materials of small volumes can only be used for estimating elastic or elastoplastic behaviors of intact rock materials. For fractured rocks, data obtained from such laboratory tests are not adequate for proper design and evaluation of the rock engineering projects if irregular fracture system geometry needs to be considered.
(6) The results show merely a conceptual understanding, since the 2D models adopted many assumptions. But the investigation provided a proper and workable tool for evaluating the impacts of anisotropy of strength and deformability of fractured rocks, especially when the host rocks are hard crystalline rocks such as granites. The mathematical approach developed can be extended to 3D cases straightforward without major mathematical difficulties, but significant increase of computing capacity is required.

Although these concluding remarks can help in understanding anisotropy of the deformability behavior and strength of fractured rock in general, some outstanding issues are identified for future research. Among them are the needs for more systematic investigations considering impacts of correlation between length and aperture of fractures, problems defined in a 3D space, and effects of groundwater pressure on strength and deformability of fractured rocks. Results for the continued research regarding these outstanding issues will be reported in near future.

Conflict of interest

We wish to confirm that there are no known conflicts of interest associated with this publication and there has been no significant financial support for this work that could have influenced its outcome.

References

Ajalloeian R, Lashkaripour GR. Strength anisotropies in mudrocks. Bulletin of Engineering Geology and the Environment 2000;59(3):195–9.
Amadei B. Importance of anisotropy when estimating and measuring in situ stresses in rock. International Journal of Rock Mechanics and Mining Sciences & Geomechanics Abstracts 1996;33(3):293–325.

Amadei B, Savage WZ. Anisotropic nature of jointed rock mass strength. Journal of Engineering Mechanics 1989;115(3):525–42.
Broch E. Estimation of strength anisotropy using the point-load test. International Journal of Rock Mechanics and Mining Sciences & Geomechanics Abstracts 1983;20(4):181–7.
Chen CS, Pan E, Amadei B. Determination of deformability and tensile strength of anisotropic rock using Brazilian tests. International Journal of Rock Mechanics and Mining Sciences 1998;35(1):43–61.
Chen W, Yang J, Tan X, Yu H. Study on mechanical parameters of fractured rock masses. Science China Technological Sciences 2011;54(1):140–6.
Cho JW, Kim H, Jeon S, Min KB. Deformation and strength anisotropy of Asan gneiss, Boryeong shale, and Yeoncheon schist. International Journal of Rock Mechanics and Mining Sciences 2012;50:158–69.
Gonzaga GG, Leite MH, Corthesy R. Determination of anisotropic deformability parameters from a single standard rock specimen. International Journal of Rock Mechanics and Mining Sciences 2008;45(8):1420–38.
Hoek E, Brown ET. Empirical strength criterion for rock masses. Journal of the Geotechnical Engineering Division ASCE 1980;106:1013–35.
Itasca Consulting Group, Inc.. UDEC 4.0 user's guide. Minneapolis, Minnesota: Itasca Consulting Group, Inc.; 2004.
Min KB, Jing L. Numerical determination of the equivalent elastic compliance tensor for fractured rock masses using the distinct element method. International Journal of Rock Mechanics and Mining Sciences 2003;40(6):795–816.
Morland LW. Elastic anisotropy of regularly jointed media. Rock Mechanics 1976;8(1):35–48.
Nirex (United Kingdom Nirex Limited). Data summary sheets in support of gross geotechnical predictions. Harwell, UK: Nirex report SA/97/052; 1997.
Nasseri MHB, Rao KS, Ramamurthy T. Anisotropic strength and deformational behavior of Himalayan schists. International Journal of Rock Mechanics and Mining Sciences 2003;40(1):3–23.
Noorian Bidgoli M, Zhao Z, Jing L. Numerical evaluation of strength and deformability of fractured rocks. Journal of Rock Mechanics and Geotechnical Engineering 2013;5(6):419–30.
Reik G, Zacas M. Strength and deformation characteristics of jointed media in true triaxial compression. International Journal of Rock Mechanics and Mining Sciences & Geomechanics Abstracts 1978;15(6):295–303.
Sun PF, Yu QL, Yang TH, Shen W. Numerical research on anisotropy mechanical parameters of fractured rock mass. Advanced Materials Research 2012;5(24):310–6.
Yang ZY, Chen JM, Huang TH. Effect of joint sets on the strength and deformation of rock mass models. International Journal of Rock Mechanics and Mining Sciences 1998;35(1):75–84.

Majid Noorian Bidgoli currently is a PhD student in the Department of Land and Water Resources Engineering, Engineering Geology and Geophysics Research Group, Royal Institute of Technology (KTH), Stockholm, Sweden, supervised by Professor Lanru Jing. His research focuses on numerical modeling of fractured rock masses using discrete fracture network (DFN) method and discrete element method (DEM) to investigate strength and deformability of fractured rocks. His interests are studying about coupled thermo-hydro-mechanical (THM) processes analysis in fractured rock masses, and also design, performance and safety assessments of slopes, foundations and underground excavations located in rock and fractured rock mass.